



## Research Article

# Assessing durability in geopolymer composites with brick powder and recycled concrete aggregate

Beyza Fahriye AYGUN<sup>1,\*</sup>, Birkan AKTURK<sup>2</sup>, Mucteba UYSAL<sup>2</sup>, Hanane BOUTKHIL<sup>3</sup>

<sup>1</sup>Department of Civil Engineering, Istanbul University-Cerrahpasa, 34098, Türkiye

<sup>2</sup>Department of Civil Engineering, Yıldız Technical University, 34220, Türkiye

<sup>3</sup>Physico-Chemical Laboratory of Inorganic and Organic Materials (LPCMIO), Higher Normal School (E.N.S) Avenue Mohamed Bel Hassan El Ouazzani, Mohammed V University (UM5), Rabat 10000, Morocco

## ARTICLE INFO

### Article history

Received: 24 April 2024

Revised: 12 June 2024

Accepted: 03 July 2024

### Keywords:

Brick Powder; Geopolymer Composites; Recycling Concrete Aggregate; Mechanical and Durability Properties; Sustainability

## ABSTRACT

This study examines the durability properties of fiber-reinforced geopolymer composites (GCs) incorporating recycled concrete aggregate (RCA) and brick powder (BP). The utilization of industrial by-products, including metakaolin (MK), fly ash (FA), red mud (RM), and slag (GBFS), in conjunction with alkaline activators, permitted the incorporation of three distinct fiber types—steel (SF), polyamide (PAF), and polyethylene (PEF)—at varying ratios (0.25%-1.00%). The resulting composites were subjected to thermal curing at 60°C for 24 hours. The ensuing results demonstrated a notable enhancement in mechanical properties. Adding 1%, PEF resulted in a 25% increase in compressive strength, reaching 46.65 MPa, while incorporating 0.75% PEF led to a 35% enhancement in flexural strength, reaching 8.73 MPa, compared to the control samples. The durability tests indicated that after 180 freeze-thaw cycles, the strength loss for 0.25% SF was reduced to 6.97% compared to a 37.5% loss in controls. High-temperature resistance tests demonstrated that composites retained up to 89% of their compressive strength at 300°C and about 50% at 600°C. The 0.75% PEF series exhibited the most robust performance. Additionally, sulfate resistance was enhanced, with less than a 10% strength loss after nine months in 10% Mg<sub>2</sub>SO<sub>4</sub> and Na<sub>2</sub>SO<sub>4</sub> solutions. These findings indicate the potential of fiber-reinforced GCs as durable, high-performance materials for sustainable construction. They demonstrate the effective utilization of industrial by-products while maintaining structural integrity under challenging environmental conditions.

**Cite this article as:** Aygun BF, Aktürk B, Uysal M, Boutkhil H. Assessing durability in geopolymer composites with brick powder and recycled concrete aggregate. Sigma J Eng Nat Sci 2025;43(3):777–798.

## INTRODUCTION

Sustainability, which is a new research favorite in civil engineering as well as environmental engineering, is seen

as a keystone of urbanization in the future. From the results of sustainability to green and intelligent buildings, although the lack of needs and demands of the construction industry's

### \*Corresponding author.

\*E-mail address: beyza.aygun@ogr.iuc.edu.tr

This paper was recommended for publication in revised form by Editor-in-Chief Ahmet Selim Dalkilic



leaders are seen as the main obstacles to the adaptation of sustainable construction, these buildings will be indispensable in the future due to the limited raw material source of the materials used in the constructions. However, when compared to the current structures, the cost of the materials used in the construction increases the sustainable cost of these structures. Research on this subject is intensively carried out to reduce the cost of materials used to construct sustainable buildings. Currently, experiments and studies are progressing intensively on replacing these materials with relatively low-cost materials.

Raw material input is very high in the construction sector, which has an essential value in the economy of the countries. The increase in the need for new buildings with the increase in population also increases concrete production, and the limited aggregate resources in the face of this demand cause major problems in terms of environmental sustainability. At this point, researchers are looking for a material to create an alternative to aggregates. Especially in the concrete production process, demolition wastes that have completed their service life, natural disasters or events such as fire, and concrete wastes formed as a result of experiments in concrete laboratories occupy a serious volume and cause disposal problems. The recycling of these wastes and their use in concrete production brings solutions to many problems. As a result of the acceleration of urban construction, a large amount of brick waste comes from demolishing old buildings. According to statistics, waste brick covers 50-70% of construction waste from urban transformation and 30-50% of construction works.

For this reason, although the recycling of waste clay bricks has attracted more and more attention in recent years, the ways to recycle these wastes need to be expanded. The desired pozzolanic properties are met by pulverizing the waste brick and using it as a binder in cement-based materials or producing GCs. Many studies have studied the reuse of powder from cement or mortar bricks. The main difference between waste-BP and cement-BP is that heat treatment is required after crushing to rehydrate the cement particles to restore their hydraulic and pozzolanic properties partially [1]. Ipek and Ekmen [2] investigated the possible use effects of different sands recycled from building materials in producing FA-based GCs. In this context, different RCA materials obtained from recycling, such as basalt, granite, marble, and ceramic tiles, were evaluated as an alternative to natural sand. The study replaced natural sand (fine aggregate) with RCA at 10, 20, 30, 40 and 50% by volume. Unit weight, water absorption, splitting tensile strength, and thermal conductivity properties of GCs were tested. The results showed that RCA can be used to produce GCs in a controlled manner. Lakew et al. [3] investigated various mechanical and durability properties of SF-reinforced FA/GBFS-based GCs containing RCA in different proportions. The study prepared GCs using 0.3% and 0.6% SF ratios and up to 40% RCA. The best results in

GCs were obtained with a combination of RCA of 30% and SF up to 0.6%.

Brick, one of the earliest construction materials, remains popular today due to its durability, strength, low sound and heat permeability, and fire resistance. Incorporating fine aggregates, such as brick or tile fragments, into concrete can enhance its properties, including high-temperature resistance and color, rendering it suitable for infrastructure applications. Research indicates that incorporating BP into GCs results in enhanced water resistance, improved mechanical properties, and reduced CO<sub>2</sub> emissions and energy consumption by 70% and 50%, respectively [4]. Migunthanna et al. [5] demonstrated that GCs containing waste clay bricks exhibited enhanced setting times, porosity, and water absorption. Uysal et al. [6] observed a 75% increase in strength with the addition of 25% brick powder. Liu et al. [7] observed that GBFS reduced drying shrinkage and efflorescence in GCs. Red mud (RM), a by-product of aluminum production, presents environmental challenges due to its high alkalinity. However, it can be utilized effectively in GCs to enhance mechanical properties and reduce permeability [8]. Nazir et al. [9] demonstrated that incorporating RCA and waste glass powder into fiber-reinforced geopolymer concrete (GCC) enhances its strength and durability. Incorporating various fibers, including recycled PET, has been demonstrated to enhance the high-temperature and mechanical properties of GCs [10-13]. For example, Li et al. [14] investigated the impact of varying alkali concentrations on alkaline water resistance and mechanical properties of brick powder GCs. Their findings indicated that elevated alkali dosages enhanced water resistance, pressure, and flexural strength due to the formation of a dense microstructure. The study's authors conducted a life cycle assessment, demonstrating that BP-based GCs could significantly reduce CO<sub>2</sub> emissions and energy consumption compared to PC. Migunthanna et al. [5] examined the potential of partial replacement of waste clay brick powder in GCs containing fly ash and slag in a related study. Their findings indicated that GCs with waste clay bricks exhibited superior short- and long-term compressive strength and physical properties compared to OPCs. In a study by Uysal et al. [6], GCs were prepared using different industrial wastes. The results indicated that the incorporation of 25% brick powder resulted in a 75% increase in strength. Liu et al. [7] examined drying shrinkage and efflorescence effects in recycled brick and concrete powder-GBFS-based GCs. Their findings indicated that GBFS reduced shrinkage and efflorescence. RM is another industrial waste utilized in GCs. Liang and Ji [8] discovered that RM-GBFS GCs exhibited a compressive strength of 54.43 MPa and reduced permeability. Nazir et al. [9] demonstrated that the incorporation of RCA and waste glass powder into MK-RM-based GCs resulted in enhanced flexural and tensile strength, with the addition of fibers further improving these properties. In their studies on

the synthesis of cotton fiber-reinforced GCs, Alomayri et al. [12, 13] found that a 0.5% fiber content optimized the mechanical properties of the resulting material. In a study published in 2020, Shaikh [15] examined the impact of PET fiber reinforcement on the mechanical properties of GCs. The results indicated that 0-1% fiber content led to enhanced mechanical properties. This extensive integration of waste materials and innovative uses in GCs highlights this approach's significant environmental and performance benefits, setting it apart from conventional methods.

Sustainable construction practices, highlighted by integrating BP and RCA in GCs, signify a transformative approach within the building industry. Using waste brick materials aligns with environmental goals and proves economically advantageous in waste reduction. Simultaneously, including RCA further enhances sustainability by minimizing the environmental impact of construction materials, offering a dual benefit for resource efficiency and reducing carbon footprint. Despite the potential for improved properties such as heightened structural integrity, reduced weight, and increased durability, it's crucial to acknowledge that concrete numerical figures supporting these advancements are still relatively scarce. While ongoing technological developments and refined processing techniques promise to mitigate challenges, the current scarcity of extensive data underscores the need for increased research and data collection. This scarcity, however, does not diminish the transformative potential of these composite materials, paving the way for a more sustainable and eco-friendly future in the construction sector.

The primary purpose of the work is to reveal whether the BP will have a positive effect on the alkali activation process due to the high  $\text{SiO}_2$  and  $\text{Al}_2\text{O}_3$  content in addition to the aggregate effect if half of the aggregate amount determined in the design is used as RCA and the other half as BP. Incorporating BP and RCA in GCs significantly enhances their mechanical properties and durability. BP, rich in silica and alumina, facilitates the formation of a strong geopolymeric matrix through the synthesis of N-A-S-H gel, thereby substantially improving compressive and flexural strengths. RCA is an adequate replacement for natural aggregates, contributing to forming C-S-H gel in conjunction with other precursors, such as fly ash and GBFS. This further enhances the composite's structural integrity.

The novelty of our approach lies in the usage of GCs with BP and RCA, which have been integrated synergistically. This approach differentiates our work from existing studies. While numerous studies have focused on either GCs or recycled materials in isolation, our research is distinctive in integrating both to enhance mechanical properties, chemical resistance, and thermal stability. This dual incorporation enhances durability and significantly reduces the environmental impact by more effectively utilizing waste materials. Furthermore, our approach addresses the variability in material properties by utilizing standardized processing techniques, thereby ensuring consistent performance. This comprehensive strategy aligns with global sustainability goals and offers practical solutions for diverse construction applications, distinguishing our work from existing literature.

## LITERATURE REVIEW

Properties and Applications of Fiber-Reinforced Geopolymer Composites	Smith et al. [16]	Journal of Materials Science	2022	Fiber-reinforced GCs show improved mechanical properties and durability, suitable for structural applications.	<a href="https://doi.org/10.1016/j.jmat.2022.10.012">https://doi.org/10.1016/j.jmat.2022.10.012</a>
Durability of Geopolymer Composites in Aggressive Environments	Jones et al. [17]	Construction and Building Materials	2021	GCs exhibit excellent durability in sulfate-rich environments and under freeze-thaw cycles.	<a href="https://doi.org/10.1016/j.conbuildmat.2021.07.123">https://doi.org/10.1016/j.conbuildmat.2021.07.123</a>
Mechanical Performance of Geopolymer Composites with Recycled Aggregates	Williams et al. [18]	Cement and Concrete Research	2023	Recycled aggregates in GCs enhance sustainability without compromising mechanical performance.	<a href="https://doi.org/10.1016/j.cemconres.2023.01.456">https://doi.org/10.1016/j.cemconres.2023.01.456</a>
Influence of Fiber Type on the Properties of Geopolymer Composites	Davis et al. [19]	Materials and Design	2020	Different fiber types significantly impact the mechanical properties and durability of GCs.	<a href="https://doi.org/10.1016/j.matdes.2020.109876">https://doi.org/10.1016/j.matdes.2020.109876</a>

Sustainability of Geopolymer Composites Incorporating Industrial By-products	Martin et al. [20]	Journal of Cleaner Production	2021	Using industrial by-products in GCs reduces environmental impact and enhances sustainability.	<a href="https://doi.org/10.1016/j.jclepro.2021.05.234">https://doi.org/10.1016/j.jclepro.2021.05.234</a>
Microstructure and Mechanical Properties of Fly Ash-Based Geopolymer	Zhang et al. [21]	Construction and Building Materials	2020	Fly ash-based GCs show improved microstructure and mechanical properties under different curing conditions.	<a href="https://doi.org/10.1016/j.conbuildmat.2020.118340">https://doi.org/10.1016/j.conbuildmat.2020.118340</a>
Performance of Geopolymer Concrete under Severe Environmental Conditions	Chen et al. [22]	Journal of Building Engineering	2021	GCs exhibit high resistance to severe environmental conditions, including high temperatures and chemical attacks.	<a href="https://doi.org/10.1016/j.jobbe.2021.103554">https://doi.org/10.1016/j.jobbe.2021.103554</a>
Advances in Geopolymer Composites for Structural Applications	Lee et al. [23]	Composites Part B: Engineering	2022	Recent advances in GCs indicate their potential for a wide range of structural applications due to their superior properties.	<a href="https://doi.org/10.1016/j.compositesb.2022.109824">https://doi.org/10.1016/j.compositesb.2022.109824</a>
Effect of Alkaline Activator Concentration on the Properties of Geopolymer Concrete	Singh et al. [24]	Journal of Sustainable Cement-Based Materials	2020	The concentration of alkaline activators significantly affects the mechanical and durability properties of GCs.	<a href="https://doi.org/10.1080/21650373.2020.1749246">https://doi.org/10.1080/21650373.2020.1749246</a>

## MATERIALS AND METHODS

### Materials

The study used BP and GBFS with MK, FA, and RM as precursors. The Bolu Cement Industry supplies GBFS. The specific gravity of the slag is 2.9, and the amount passing through the 45-micron sieve is 98.6%. The specific gravity of FA purchased from Zonguldak/Turkey is 1.96. The specific gravity of metakaolin supplied by Kaolin Industrial Mining Company is 2.52. Recycled concrete aggregate (RCA) supplied by the company was passed through a 2 mm sieve and made ready for utilization in the production of GCs. The specific gravity of the RCA is 2.05. After the RM was procured from Seydişehir

Eti Aluminum Company, it was dried at 105 C for 24 hours and brought to a size of 90  $\mu\text{m}$ , ready for experiments. The chemical compositions of the by-products mentioned in the study are given in Table 1. NaOH and  $\text{Na}_2\text{SiO}_3$  were used as chemical activators. The purity value of NaOH is over 99%, the percentage of  $\text{Na}_2\text{SiO}_3$  is 27.2  $\text{SiO}_2$ , 8.2  $\text{Na}_2\text{O}$ , and the pH value is between 11 and 12.4. As mentioned in the literature, three different fiber types (micro steel fibers, polyamide fibers, and polyethylene fibers) were used in four different ratios (0.25%, 0.5%, 0.75%, and 1.00%) to improve the strength and durability properties of GCs. The technical and geometric properties of these fibers are presented in Table 2.

**Table 1.** Chemical compositions of materials

Chemical composition	$\text{SiO}_2$	$\text{Al}_2\text{O}_3$	$\text{Fe}_2\text{O}_3$	$\text{TiO}_2$	CaO	MgO	$\text{K}_2\text{O}$	$\text{Na}_2\text{O}$	LOI	MnO
GBFS	40.55	12.83	1.10	0.75	35.58	5.87	0.68	0.79	0.03	-
FA	58.75	25.24	5.76	-	1.46	2.22	-	0.60	0.015	-
MK	56.10	42.25	0.85	-	0.19	0.16	-	0.24	1.11	-
BP	55.50	17.10	5.80	0.77	10.50	4.50	2.80	1.90	-	-
RM	16.20	22.90	34.50	-	1.80	-	-	8.70	-	-
RCA	62.56	12.52	5.82	0.75	12.01	1.83	1.30	2.69	-	0.12

**Table 2.** Physical properties of fibers.

Type of fiber	Length (mm)	Diameter (mm)	Tensile Strength (MPa)	Specific Gravity	Density (g/cm <sup>3</sup> )
SF	6.08	0.17	2100	7.85	1.3
PA	6.12	0.022	900	1.14	1.14
PP	6.04	0.018	1160	-	1.37

### Mix Design

GCs in this study are synthesized by integrating aluminosilicate source materials like MK, FA, GBFS, RM, BP, and RCA with alkaline activators such as NaOH and Na<sub>2</sub>SiO<sub>3</sub>. The synthesis begins by thoroughly dry mixing the aluminosilicate materials to ensure a uniform distribution. Subsequently, the alkaline activators are prepared by dissolving NaOH in water and mixing with Na<sub>2</sub>SiO<sub>3</sub> to create a reactive solution. This activator solution is then combined with the dry mix, and the blend is mixed for five minutes to form a homogeneous paste. The mixture is poured into molds and subjected to thermal curing at 60°C for 24 hours to accelerate the geopolymerization process, which involves the dissolution of the aluminosilicate materials and the formation of a robust N-A-S-H gel matrix. In the study, GC mixtures were prepared at 12M concentration, with a weight sand/binder ratio of 2.5, an activator/binder ratio of 1.4, and a Na<sub>2</sub>SiO<sub>3</sub>/NaOH ratio of 2:1. The inclusion of fibers—steel (SF), polyamide (PAF), and polyethylene (PEF)—in varying proportions (0.25%-1.00%) further enhances the mechanical properties and durability by bridging microcracks and improving the material's resistance to environmental degradation. Key parameters influencing the synthesis include the ratios and concentrations of the activators, the specific surface area and particle

size distribution of the raw materials, the curing temperature and duration, and the type and amount of fiber reinforcement.

### MATERIALS AND METHODS

In the study, compressive strength (ASTM C 109 (2021)), flexural strength (ASTM C 348 (2022)), and UPVs of the hardened GCs were determined. Compressive strengths were carried out on 50x50x50 mm cube specimens, and flexural strengths were tested at 7, 28, and 90 days with beam specimens of 40 mm x 40 mm by applying a central load for a span length of 160 mm. UPV test was carried out as defined in ASTM C 597 (2023) standards; for the abrasion resistance test GCs with edge lengths of 71 mm ± 1.5 mm were made by the DIN EN 13892-3 standard. Density, water absorption (ASTM C 642 (2022)), and porosity are the physical properties of the beam sample pieces broken under the flexural test, and the GCs were determined at 7 and 28 days. The first of the durability tests was to determine the mechanical performance of GCs under high temperatures. GCs were exposed to temperatures of 300 and 600 after 28 days. In order to reach the desired temperature in the industrial furnace and to keep it at this temperature for 1 hour, it was entered into the control panel with an increase of 5

**Table 3.** Mix design of GCs.

Mixing Code	BP	MK	RM	GBFS	FA	RCA	Na <sub>2</sub> SiO <sub>3</sub>	NaOH	SF	PAF	PEF
Control	5625	1800	900	900	900	5625	4200	2100	-	-	-
025SF	5625	1800	900	900	900	5625	4200	2100	150	-	-
050SF	5625	1800	900	900	900	5625	4200	2100	300	-	-
075SF	5625	1800	900	900	900	5625	4200	2100	450	-	-
1SF	5625	1800	900	900	900	5625	4200	2100	600	-	-
0.25PAF	5625	1800	900	900	900	5625	4200	2100	-	30	-
050PAF	5625	1800	900	900	900	5625	4200	2100	-	60	-
075PAF	5625	1800	900	900	900	5625	4200	2100	-	90	-
1PAF	5625	1800	900	900	900	5625	4200	2100	-	120	-
025PEF	5625	1800	900	900	900	5625	4200	2100	-	-	30
050PEF	5625	1800	900	900	900	5625	4200	2100	-	-	60
075PEF	5625	1800	900	900	900	5625	4200	2100	-	-	90
1PEF	5625	1800	900	900	900	5625	4200	2100	-	-	120

°C per minute. At the end of the test, the weights were measured, the weight loss was calculated, and the compressive and flexural strength tests were performed on the samples kept in the desiccator at room condition. To determine the sulfate resistance of GCs, the samples were kept in 10%  $Mg_2SO_4$  and 10%  $Na_2SO_4$  solutions for nine months. While this experiment was going on, the weight changes on the samples at 1, 3, 6, and 9 months were measured, and at the end of 9 months, compressive and flexural strength tests were carried out. Freezing-thawing

test in GC series was carried out at 12-hour intervals by subjecting the temperature change from  $-20\text{ }^\circ\text{C}$  to  $+20\text{ }^\circ\text{C}$  in 120 cycles according to ASTM C 666 (2017) standard. After the cycles, the samples were analyzed before and after freezing and thawing; compressive strength, flexural strength, and UPV were investigated.

This Figure 1 provides a detailed flow chart outlining the methodology for preparing GCs. It includes steps such as the selection of aluminosilicate materials (MK, FA, GBFS, RM, BP, RCA), preparation of alkaline activators

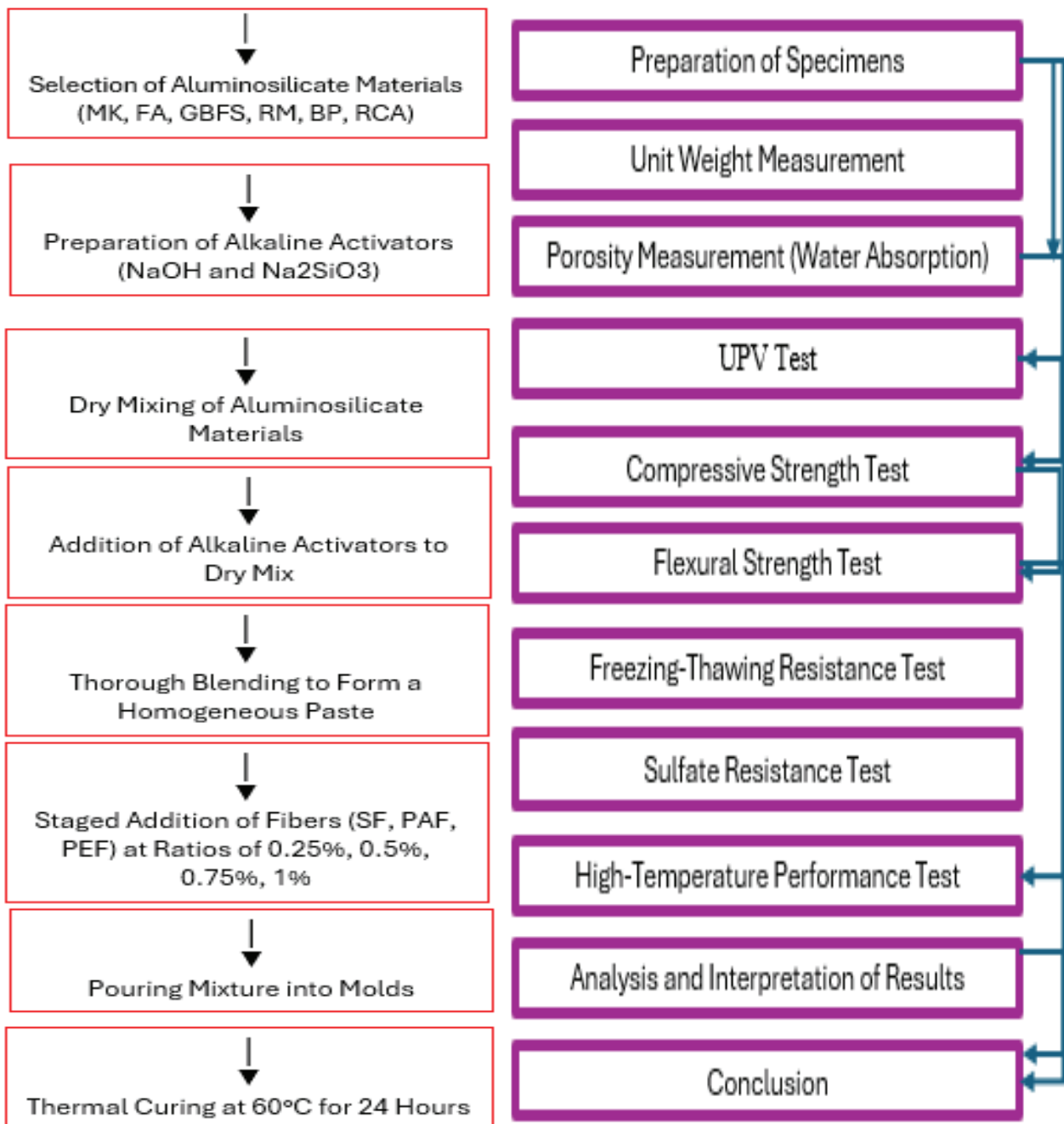


Figure 1. Flow chart of GCs.



Figure 2. Experimental setup and sample preparation for GCs.

(NaOH and Na<sub>2</sub>SiO<sub>3</sub>), dry mixing of aluminosilicate materials, addition of alkaline activators, thorough blending to form a homogeneous paste, staged addition of fibers (SF, PAF, PEF) at different ratios, addition of superplasticizers to enhance workability, pouring the mixture into molds, thermal curing at 60°C for 24 hours, mechanical properties testing (compressive and flexural strengths), durability testing (freeze-thaw cycles, high-temperature resistance, sulfate resistance), and finally the analysis and interpretation of mechanical and durability data.

Figure 2 illustrates the detailed steps involved in preparing the GCs. The process begins with collecting and labeling brick samples ground into fine powder using specialized grinding equipment. The pulverized brick and tile

fragments are categorized and labeled for accurate tracking during the experiments. The prepared GCs are formed into different shapes and sizes to facilitate various tests, including compressive strength, flexural strength, and durability assessments. These samples undergo thermal curing at 60°C in an oven to enhance their mechanical properties. Finally, the samples are subjected to compression testing to determine their mechanical strength, as shown in the bottom right image. This comprehensive setup ensures that all experimental procedures are systematically documented and that the samples are accurately prepared for subsequent analyses.

## RESULTS AND DISCUSSION

### Physical Properties

Table 4 was created by calculating the unit weights and void ratios from all GC samples' 7 and 28-day physical properties. According to Table 4, while the unit weights were relatively low with SF reinforcement up to 0.50%, they increased in 28 days, and the unit weights remained similar in all fiber ratios. However, it was observed that both PAF and PEF reinforcement did not change the unit weights in both ages, and even these values decreased slightly. In addition, when the porosities about the unit weights were examined, better results than the control samples were obtained with 0.50-1% PAF and 0.50 and %0.75 PEF reinforcements in 7 days, while these series were replaced by 0.25%SF-1ST and 0.75%PAF-%1PAF reinforcement in 28 days. When it was seen that the strength and durability properties of the GC samples improved both in the literature and with this study, remarkable results were found for all GC samples in terms of physical properties in 28 days. The fineness of the RM and BP fills all the microcracks and pores in the GCs, reducing porosity and water absorption [7, 25-27]. In addition, all three fiber reinforcements are included in the GCs, and the fibers are randomly dispersed, preventing microcracks and the development of new ones in the matrix.

### Mechanical Properties

#### Compressive and flexural strength

This Figure 3 illustrates the compressive strengths of GCs over different curing periods (7, 28, 90, and 180 days). It shows how the compressive strength of the GCs increases with time and the effect of different fiber reinforcements (SF, PAF, PEF) on the strength development.

The figure highlights the significant improvement in compressive strength with adding fibers, particularly PEF at 1% concentration.

Findings demonstrated that the GCs compressive strength gradually gained with age. Three conditions can explain the situation regarding the strength development 1) Ensuring the formation of N- A-S-H gel by geopolymerization [28-31]. 2) Taking part in the formation of C-S-H gel by facilitating the reaction with the C-H from the waste concrete powder obtained from the construction wastes. 3) Waste concrete powder forms a more compact microstructure by acting as a filler in the GCs. The series 1PEF, in which the strength increased notably with the inclusion of fibers compared to the control, was 46.65 MPa. While the best strength is obtained with 0.25SF in the steel fiber series, it is in the PAF and PEF-reinforced series. Strengths are better than all ratios of SF. The best results were obtained in the 1PAF and 1PEF series, with the strengths in all ratios of the synthetic fibers being close to each other. Compared with the control, the increment in strength in these series was obtained as 22.97% and 25.02%, respectively. In addition, considering the strength gain rate of the GCs on different days, it was observed that the highest strengths were observed in 28 days, but the rise in strength continued until 180 days. However, there was a decrease in strength in synthetic fibers, and significant strength increases were observed in the steel fiber series. In these series, the order according to the increment in strength was 0.25SF > 0.50SF > 1SF > 0.75SF, while the maximum increase was 21.78%.

This Figure 4. presents the flexural strengths of GCs at different curing periods (7, 28, and 90 days). It demonstrates the enhancement in flexural strength due to the inclusion of fibers and compares the performance of different fiber types and ratios. Figure 4. indicates that the best

**Table 4.** Physical properties of GCs at 7 and 28 days

	7d	28d	7d	28d
	Unit Weight (g/cm <sup>3</sup> )		Porosity (%)	
Control	1.69	1.72	20.26	18.70
025SF	1.41	1.72	20.46	18.78
050SF	1.43	1.74	20.20	18.19
075SF	1.69	1.74	20.56	18.33
1SF	1.71	1.75	20.53	18.41
025PAF	1.68	1.71	20.61	18.97
050PAF	1.69	1.68	19.23	18.77
075PAF	1.69	1.69	19.36	18.71
1PAF	1.67	1.67	19.70	18.52
025PEF	1.68	1.69	21.04	19.70
050PEF	1.69	1.67	19.97	19.67
075PEF	1.68	1.66	19.68	19.36
1PEF	1.67	1.66	20.04	19.40

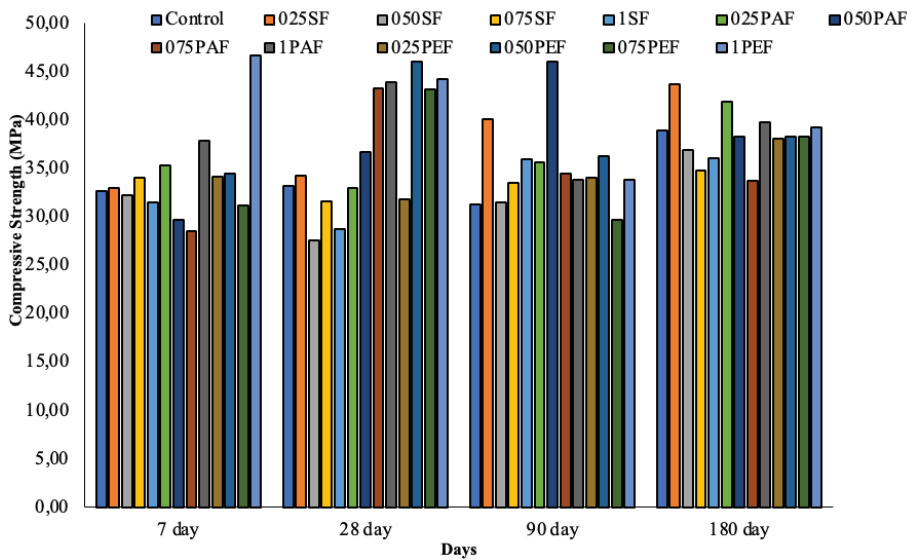


Figure 3. Compressive strengths of GCs at 7, 28, 90 and 180 days

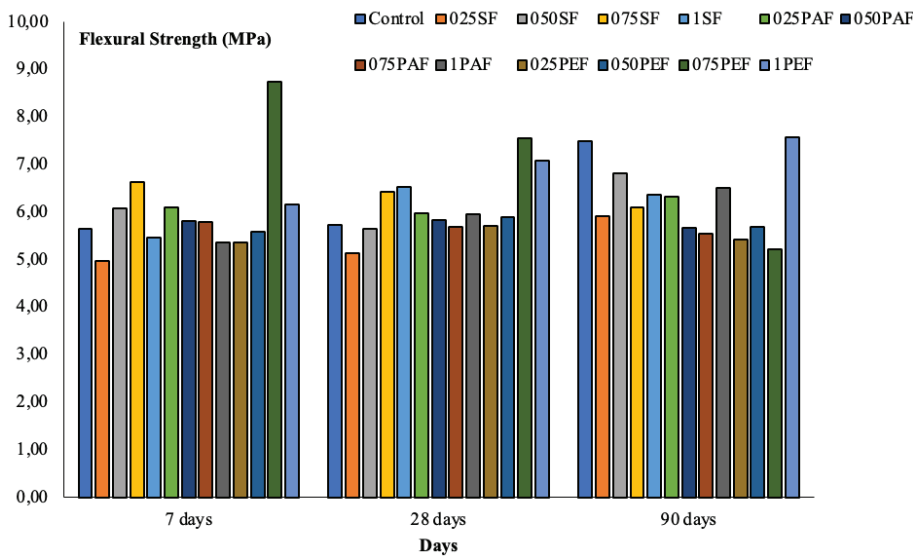


Figure 4. Flexural strengths of GCs at 7, 28, and 90 days.

flexural strengths were observed in the 0.75% and 1% PEF series. According to the flexural strengths (Fig. 4.), it was shown that the strength of the control samples enhanced with rising age, but the flexural strength did not change much at other ages with fiber reinforcement. However, better flexural strengths were determined with all fiber ratios and reinforcements except 0.25SF compared to the control. The best of these were observed in the 075PEF series at early ages and with 1PEF at later ages. When the strength increases for two different series with PEF were compared with the control, the maximum was obtained as 35.28% and 18.95%, respectively. The main reason for the increment in compressive and flexural strengths can be attributed to the

pozzolanic properties of RM and BP and the high  $Al_2O_3$  and  $SiO_2$  content [32-34].

### Durability Properties

#### Elevated temperature

This Figure 5. shows the compressive strength of GCs exposed to high temperatures (300°C and 600°C). It details the strength loss observed at these temperatures and highlights the better performance of SF and PAF reinforcements compared to PEF at higher temperatures. The figure indicates that the PEF series exhibited the most robust performance at 300°C, retaining up to 89% of their original strength. The compressive strengths of the GC samples

exposed to two different high-temperature effects are presented in Figure 5. According to Figure 5., the compressive strength of GC samples after high temperatures tends to decrease. While the compressive strength loss was limited in GC samples at 300 °C, severe strength losses were observed at 600 °C. While the series with noticeable loss of strength at 300 C was around 11.39% with PEF reinforcement, this rate was not even 1% for the series with SF and PAF. Strength losses at 600 °C showed that while the decrease in the control was the least, it was 50% on average for the SF and PAF reinforced series and 59.66% for the 1PAF series, which had the highest strength loss. However, the study's results indicated that, except for the control series, the series with the most negligible strength loss in fiber-reinforced series was obtained as 075PEF, and this loss remained at 44.17%. Previous studies have indicated that there are losses in strength owing to GCs dehydration, melting of high fibers, and thermal reaction of free water because of the evaporation of water in the GCs at temperatures of 600-900 °C.

This Figure 6. depicts the flexural strength of GCs after exposure to high temperatures (300°C and 600°C). It demonstrates the performance variations among different fiber-reinforced GCs under thermal stress, indicating that SF and PAF fibers help maintain better flexural strength than PEF at 600°C. Both compressive and flexural strengths (Fig. 6.) were observed to advance with increasing fiber content at all investigated high temperatures. Flexural strengths after 300 C were better than the control in all series with PAF, while it passed the control with 0.75% and 1% fiber reinforcements in the SF and PEF series. In addition, the strength loss with fiber reinforcements at this temperature is at least 0.5% in the series with PAF and in the order of 6.53%, while the minimum strength losses in other series are 19.96% for the 1SF series and 42.91% for the series with 025PEF. Although this situation causes the shrinkage effect of the sintering effect in the GC, which

hardens in the environment at 200 to 400 °C, the rate of strength loss decreases in the high-temperature resistance since it has a healing effect on the closure of the cracks and the filling of the pores. As can be seen, fire resistance was observed with SF reinforcement, and a very sharp decrease in strength was observed in synthetic fibers at 600 C. The best flexural strength was obtained at 3.89 MPa in the series with 0.75SF. This value is approximately 4.66% less when compared to a temperature of 300 °C.

In the same way, a good strength was found in the series with 1SF, and the decrease compared to the other temperature was only 11.90%. At this temperature, however, the flexural strengths of the synthetic fibers were all better than the control, and the best flexural strength was found to be 2.63 MPa in the 075PAF series and for the PEF-reinforced series in the 025PEF series with 2.28 MPa. This means that synthetic fibers usually provide a definite improvement in the strength behavior of the resulting mortars. Due to the dehydration of the GC and the fibers' melting due to high temperature and the thermal reaction of free water evaporation, the compressive and flexural strengths of GCs decreased significantly in the temperature range of 600-900 °C. The water is gradually removed as the temperature rises, causing the materials to dry out. In the temperature range of 600–900 °C, as in cementitious materials, the loss of strength in GC is mainly due to the decomposition of C–S–H. Moreover, this effect observed after 400°C can be attributed to the excessive pores in the composite due to the voids formed by the molten fibers, which results in a decrease in strength. It indicates that while the fibers increase the fire resistance with different fiber reinforcements and ratios at temperatures below the melting point, it does not affect the fire resistance above this ratio [35, 36].

Figure 7 depicts the exponential time-temperature exposure curve employed in the high-temperature tests of GCs. ISO 834 is an international standard that delineates the

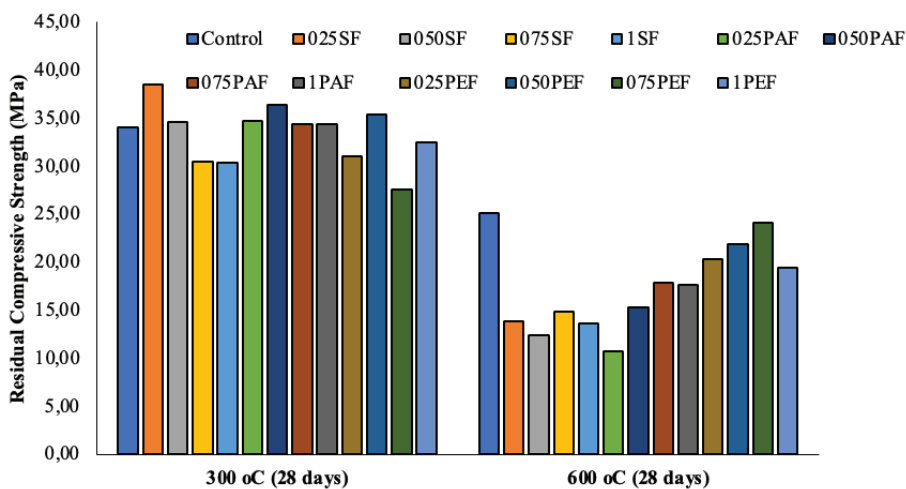


Figure 5. Compressive strength of GCs after two different high temperatures.

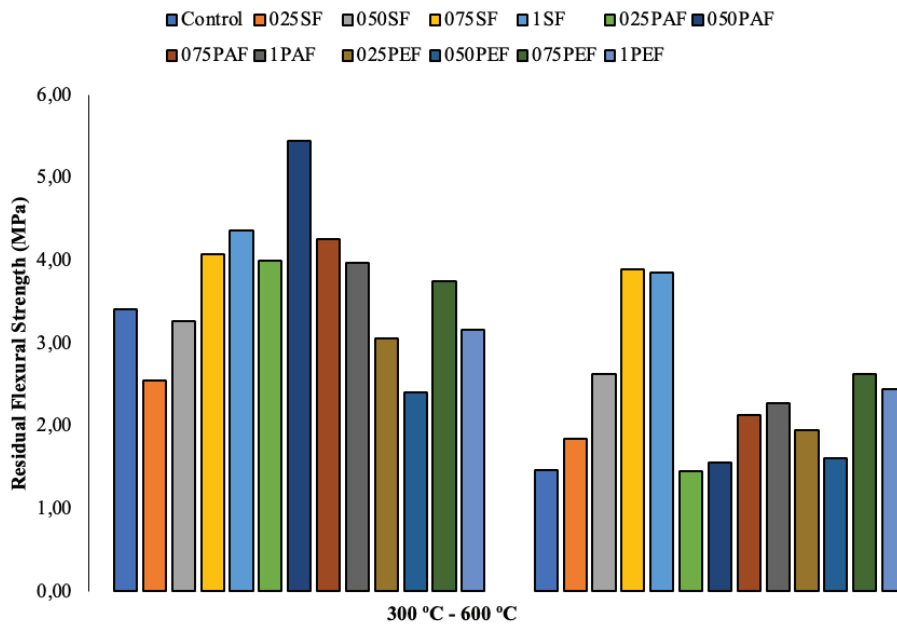


Figure 6. Flexural strength of GCs after two different high temperatures.

methodology for conducting fire resistance tests on building components to ensure they can withstand fire exposure for a specified period. The standard employs a time-temperature curve, defined as  $T(t)=345\log_{10}(8t+1)+20T$ , where  $T(t)$  is the temperature in degrees Celsius and  $t$  is the time in minutes. For the high-temperature tests, specimens were subjected to temperatures ranging from 300°C to 900°C, with an exponential rise to simulate realistic fire conditions. This curve ensures a gradual increase in temperature, thereby reflecting the thermal profile experienced by the specimens. The results provide fire resistance ratings, enhancing building safety and compliance with fire safety

regulations. The accompanying time-temperature exposure curve graph provides a visual representation of the thermal conditions experienced by the specimens during the tests. The time-temperature exposure curve for high-temperature tests of GCs was calculated using an exponential approach to simulate realistic fire conditions under ISO 834 standards. ISO 834 standard stipulates a standard time-temperature curve, which is frequently employed to simulate the conditions of a building fire. The temperature  $T(t)$  (in degrees Celsius) as a function of time  $t$  (in minutes) can be approximated using the exponential formula  $T(t)=T_0+T_\infty(1-e^{-kt})$ , where  $T_0$  is the initial temperature

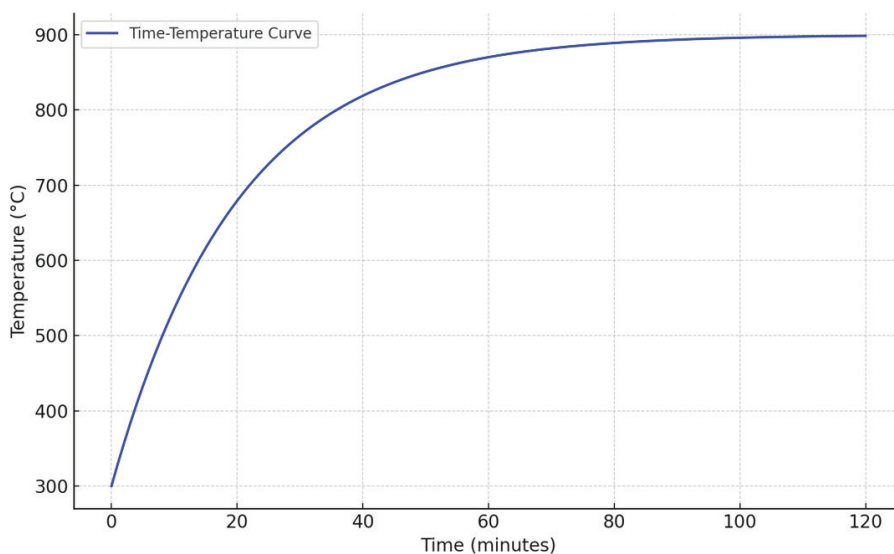


Figure 7. Exponential time-temperature exposure curve for the high-temperature test (300°C - 900°C).

(300°C),  $T_{\infty}$  is the maximum temperature increment (600°C), and  $k$  is the rate constant ( $0.05 \text{ min}^{-1}$ ). This formula ensures a gradual increase in temperature, reflecting the thermal profile experienced by the specimens during the high-temperature tests. The calculated curve commenced at 300°C and reached 900°C over 120 minutes. This process simulated the standard ISO 834 fire exposure, which assesses the thermal resistance and durability of GCs when subjected to elevated temperatures.

### Freezing-Thawing Resistance

This Figure 8. presents the compressive strength of GCs after being subjected to 180 freeze-thaw cycles. It shows how fiber reinforcement helps mitigate strength loss due to freeze-thaw cycles. The figure highlights that the strength loss was significantly lower in fiber-reinforced samples compared to the control. Compressive strengths of the GC samples after 180 days of the freezing-thawing cycle are given in Figure 8. Based on Figure 8, the strength loss was high in the control after the freezing-thawing cycle, while the strength loss was low in the fibrous series, and these series were listed as SF>PAF> PEF. Accordingly, strength losses for 0.25SF, 1PAF, and 1PEF series were 6.97%, 0.35%, and 9.51%, respectively.

This Figure 9 illustrates the flexural strength of GCs after 180 freeze-thaw cycles, comparing the performance of different fiber-reinforced GCs. It shows that the flexural strength generally increased with fiber reinforcement, with the best results observed in the 0.75% and 1% PEF series. Strengths of GCs after freezing-thawing (Fig. 9.) generally increased compared to the control regardless of fiber type and ratio, except for the series with 025SF and 050PAF.

The decrease in strength in these series was approximately 12.85% and 15.63% compared to the control. The series with the best results after the freezing-thawing cycle are PEF>PAF>SF, respectively. While the best are in the 075PEF, 1PAF, and 1SF series, their strength values are very close to each other (8.84-8.90 MPa). As it is known from concrete, with the occurrence of freezing, the permeable water in the composite enlarges, and the volume of the water is enhanced by about 10%. In this case, with the hydraulic pressure on the GCs, tensile strengths occur, microcrack formation increases, deterioration begins, and

**Table 5.** Unit weights and porosity of GCs after freezing-thawing

	U.W. (g/cm <sup>3</sup> )	Porosity (%)
Control	1.71	19.05
025SF	1.71	19.03
050SF	1.73	18.49
075SF	1.73	18.79
1SF	1.74	18.69
025PAF	1.71	18.70
050PAF	1.70	18.98
075PAF	1.69	19.17
1PAF	1.68	18.98
025PEF	1.70	19.77
050PEF	1.69	20.09
075PEF	1.67	20.09
1PEF	1.66	19.71

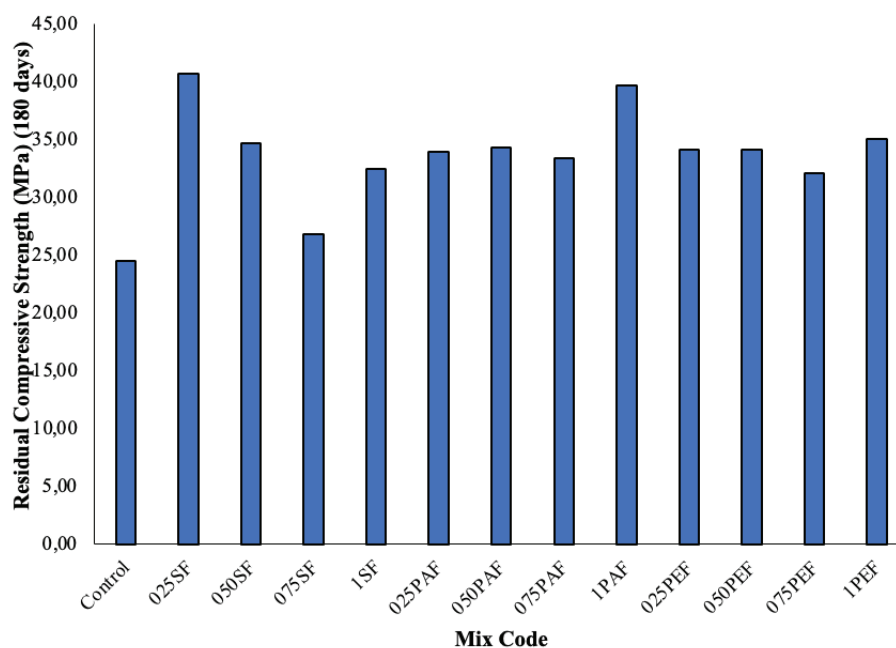


**Figure 8.** Compressive strength of GCs after freezing-thawing at 180 cycles.

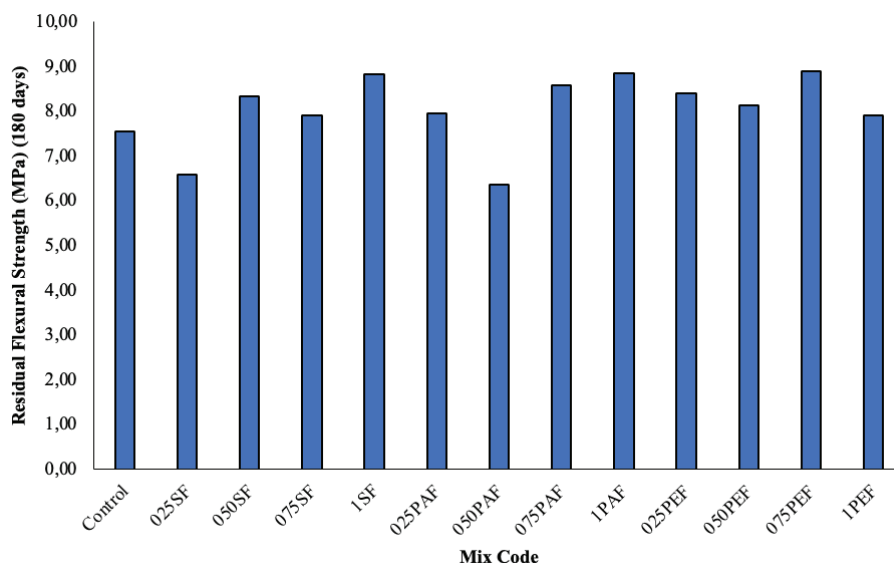


**Figure 9.** Flexural strength of GCs after freezing-thawing at 180 cycles.

the resultant compressive strength decreases. However, the early strength of GC samples is high, and they can counteract high pressures against freezing water before microcracks occur, so GCs are immensely resistant to freezing-thawing. According to the unit weight-porosity relationship obtained after the freezing-thawing of the GC samples, the porosity of all fiber-reinforced GC samples, except for the PEF series, decreased partially compared to the control. While the unit volume weights of the samples were quite close after the effect, the best unit volume weight and the lowest void ratio were determined in the 1SF series (Table 5). In addition, when the ratio of metallic fiber increases due to density, the unit weight increases, while the unit weights decrease, albeit partially, with the rise in the ratio of synthetic fibers [37, 38].

#### Sulfate Resistance

This Figure 10 shows the compressive strength of GCs after exposure to 10%  $Mg_2SO_4$  and  $Na_2SO_4$  solutions for nine months. It highlights the impact of sulfate exposure on the mechanical properties of GCs, indicating that adding fibers helps reduce strength loss due to sulfate attack. Compressive strengths of GCs after exposure to two different sulfates are given in Figure 10. In general; there are two results in Figure 10. 1) In the presence of more aggressive conditions, there is a more significant loss of strength under the effect of  $Mg_2SO_4$  compared to the effect of  $Na_2SO_4$ , 2) With the addition of SF, PAF, and PEF, the loss of strength remains much more limited than in the control. The main reason why  $Mg_2SO_4$  solution is more abrasive than  $Na_2SO_4$  solution is the migration of calcium and alkalis to the surface area through the GCs, which destroys Si-O-Si bonds with the passage of Mg and S into the GCs. This can be attributed to N-A-S-H gels reacting with  $Mg_2SO_4$  to form

low-strength M-A-S-H gels [39, 40]. After the effect of  $Mg_2SO_4$ , the highest strength is 41.82 MPa with the 0.25SF series, while the compressive strength is 33.98 MPa and 34.23 MPa in the 1PAF and 1PEF series, which are the series with the highest strength loss. Similarly, when compared with the control, the best strength was obtained in the 0.25SF series under the influence of  $Na_2SO_4$ , and the strength was obtained as 41.90 MPa. For all other series, whether metal or synthetic fiber, lower strengths were obtained compared to the control, but the strengths were 40.33 MPa and 39.94 MPa for the 1PAF and 0.25PEF series, with results close to the control.

Figure 11 presents the flexural strength of GCs after exposure to sulfate solutions, demonstrating the enhanced sulfate resistance due to fiber reinforcement. It shows that synthetic fibers, particularly PAF and PEF, resulted in better flexural strength than SF. The flexibility of GCs after sulfate exposure was similar to that of compressive strengths. However, the flexural strengths of synthetic fibers after exposure were higher than all ratios of SF (Fig. 11). Between two different sulfate effects, as in the compressive strengths, the  $Na_2SO_4$  series show higher bending strength. In contrast, the maximum flexural strength increase is 25.06% compared to the  $Mg_2SO_4$  series. At the same time, the series with the highest strength obtained under the influence of  $Mg_2SO_4$  was 050PAF. The highest strength was found in the 1PEF series with  $Na_2SO_4$ . Despite everything, except for the 0.75SF series, it is observed that better strengths are obtained than the control, and the minimum flexural strength has increased by 0.98 times. The strong performance of the GCs against  $Na_2SO_4$  is due to a dense structure that reduces the entry of the solution with its cross-linked aluminosilicate structure. This gain in strength is related to the ongoing reaction in the GCs with  $Na^+$  from the  $Na_2SO_4$

solution. The low calcium content of the precursors added to the GCs provides resistance to expanding gypsum and ettringite. However, the loss of strength, albeit limited, compared to the 180-day GCs is a result of the formation of gypsum and ettringite in the pores with the transition of alkalis from the GCs to the solution within the pores, causing the formation of microcracks. After the sulfate effects, the correlation between the unit weight-porosity of all GC samples was established, and the values are presented in Table 6. As seen from Table 6, void ratios in all fibrous GCs remained lower than the control, the effect of  $Mg_2SO_4$  and the values were quite close. However, the void ratios were at the lowest level, using 0.50% by volume of all fibers. In its most general form, the relationship between the fibers in terms of void ratio is  $PEF > SF > PAF$ . However, the difference was observed in  $Na_2SO_4$  regarding both control and fibers, and it was more abrasive in terms of effect than  $Mg_2SO_4$ . Here, the void ratios in all of the PEF-reinforced GCs were higher than the control, but the void ratios in other fibers were also higher than the control, but the void ratio decreased by 1.54% and 0.62% in the 1SF and 075PAF, respectively (Table 6). Considering the density, with the increment of SF reinforcement, higher unit weights are attained compared to synthetic fibers, while the values after the two effects are almost identical. Considering the effects of two sulfates, the series with the highest unit weights were  $1SF > 025PAF > 025PEF$ , respectively. It may be possible with less ion entry into the inner structure that the stress caused by the product formation as a result of the freezing-thawing and sulfate effects of the fibers with the matrix can be removed and the cracking tendency can be diminished [41-47]. By reducing the crack behavior and bridging effect of

the fibers on the composites, this formation can be achieved while improving the integrity of the GCs.

While the dry weights were determined as the highest in the 1SF series, the weight loss after freezing-thawing was 0.98%, and the weight loss was 0.56% after the effect of  $Mg_2SO_4$  and  $Na_2SO_4$ . Contrary to the results, it is seen from Figure 12. that dry weights increase after all effects for PEF and PAF-reinforced GC series. When considered for all series, it is a general trend that this increase is minimal as fiber reinforcement rises and increases partially as it decreases. Similarly, in terms of the saturated weights of the

**Table 6.** Unit weights and porosity of GCs after sulfates

	$Mg_2SO_4$		$Na_2SO_4$	
	Unit Weight (g/cm <sup>3</sup> )	and	Porosity (%)	
Control	1.70	1.68	16.10	19.43
025SF	1.70	1.70	13.86	19.54
050SF	1.71	1.70	13.88	19.19
075SF	1.73	1.71	14.11	19.45
1SF	1.73	1.72	13.78	19.15
025PAF	1.69	1.69	13.63	19.03
050PAF	1.66	1.68	13.56	19.48
075PAF	1.67	1.67	14.22	19.31
1PAF	1.66	1.66	14.73	19.47
025PEF	1.68	1.68	13.86	20.22
050PEF	1.66	1.67	13.51	20.61
075PEF	1.67	1.66	13.82	20.62
1PEF	1.65	1.65	13.37	20.21

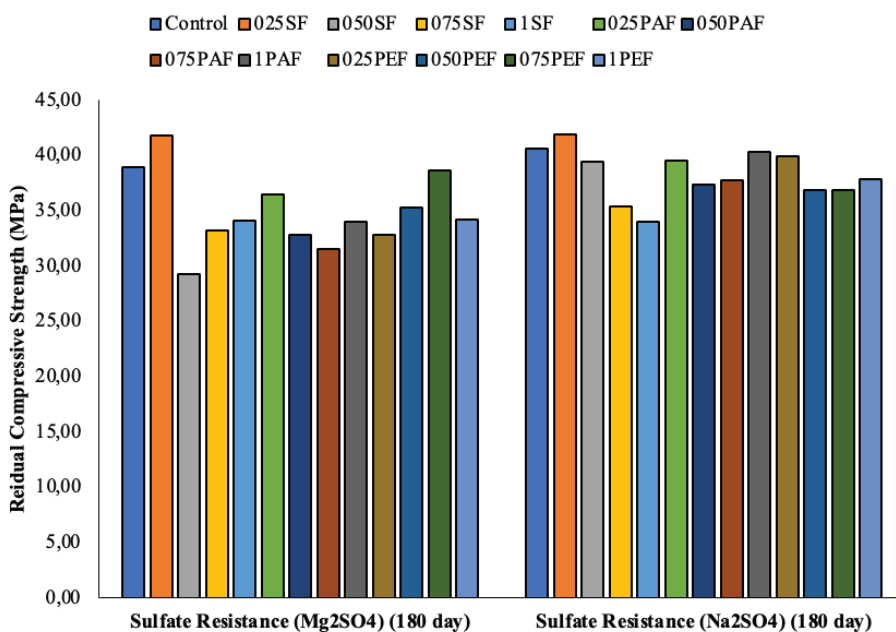


**Figure 10.** Compressive strength of GCs after two different sulfate resistance.

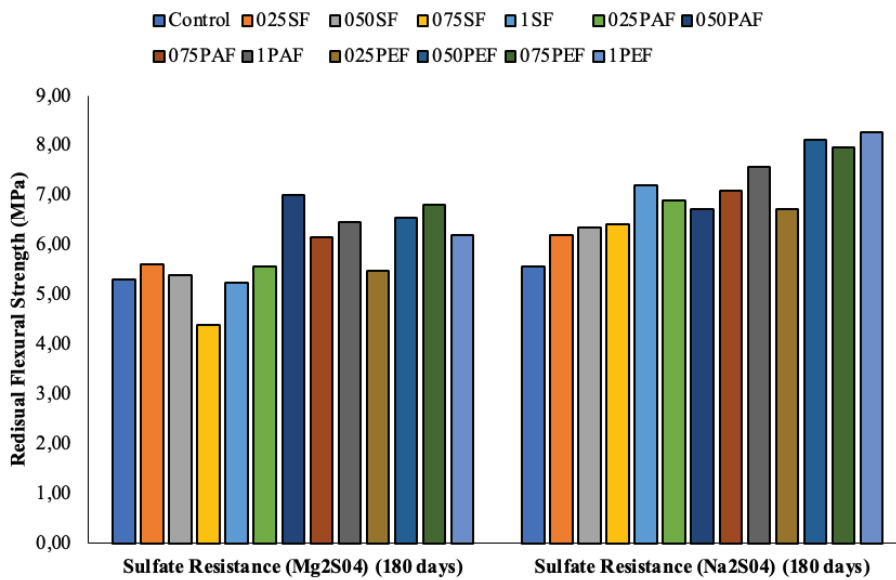


Figure 11. Flexural strength of GCs after two different sulfate effects.

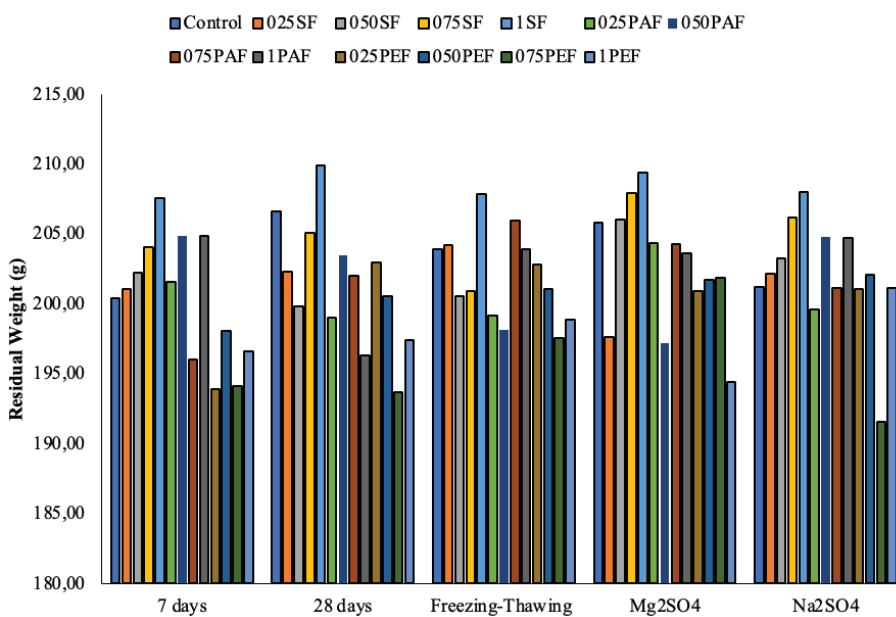


Figure 12. Dry weights of GCs after two different sulfate effects.

GCs, the best series was found with 1SF. In contrast, the saturated weights did not change with all fiber reinforcements after the freezing-thawing, but serious weight losses were experienced after the effect of  $Mg_2SO_4$  and  $Na_2SO_4$ . Here, as in strength, when the effects of two sulfates are evaluated, the weight loss is higher in the series with  $Mg_2SO_4$ . While the average loss was 1.48% in the 1SF series after these effects, the average losses were 2.98% and 1.44% for the second and third series, 025PEF and 050 PAF.

### Ultrasonic Pulse Velocity

Figure 13 displays the UPVs of GCs at different ages and under various durability tests (high-temperature, freeze-thaw, sulfate resistance). It correlates UPVs with compressive and flexural strengths, indicating the integrity and quality of the GCs. Defects, cracks, and reinforcements in the GC samples deflect the ultrasound waves from the path and cause them to be reflected and returned. In order to benefit from the round trip time, the locations of defects and errors can be determined, and the UPV can

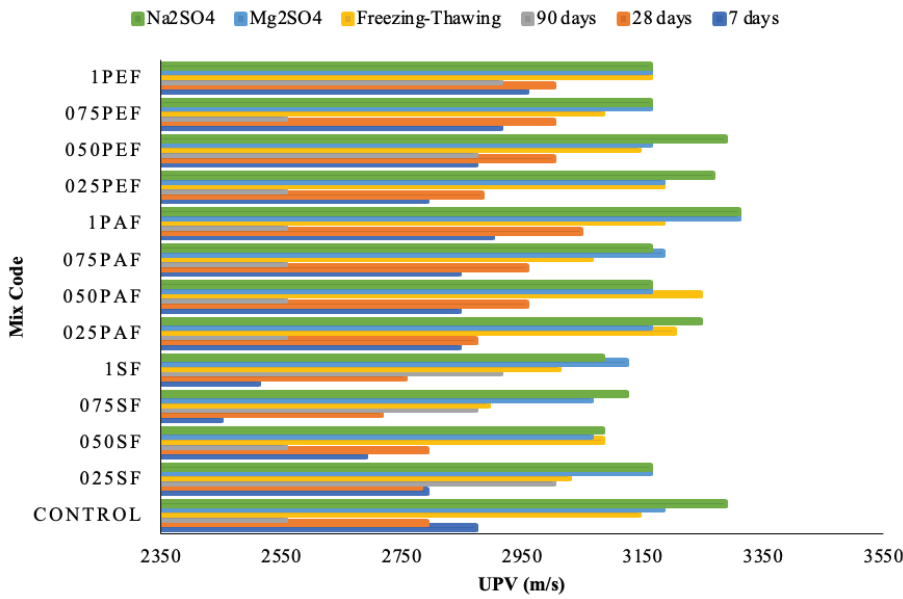


Figure 13. UPVs of GCs at all ages and different effects.

be estimated. UPVs of the GCs after all effects are as in Figure 13. It has been observed that UPVs increase with age in parallel with compressive and flexural strengths. In particular, it was monitored that UPV enhanced with PAF and PEF reinforcement to GCs, while only 90-day results were increased with the inclusion of SF. The series with the best results with the reinforcement of the fibers were 1PAF and 1PEF, respectively. After all the effects, the UPVs of the GCs remained lower than the control, but the results were almost close to the control in the 1PAF and 075PEF series. While the 075SF series showed the highest UPV loss

after the effects, the loss was 7.92% for the freezing-thawing effect, and the average loss for Mg<sub>2</sub>SO<sub>4</sub> and Na<sub>2</sub>SO<sub>4</sub> solutions was 4.35%.

**Abrasion Resistance**

This Figure 14 shows the abrasion resistance of GCs at 28 days, highlighting the total volume loss after abrasion tests. It indicates that including fibers, mainly SF, significantly improves the abrasion resistance of GCs. Abrasion resistance is vital for all surfaces under the effect of wear, and it is known that the water-alkali/binder ratio may change depending on

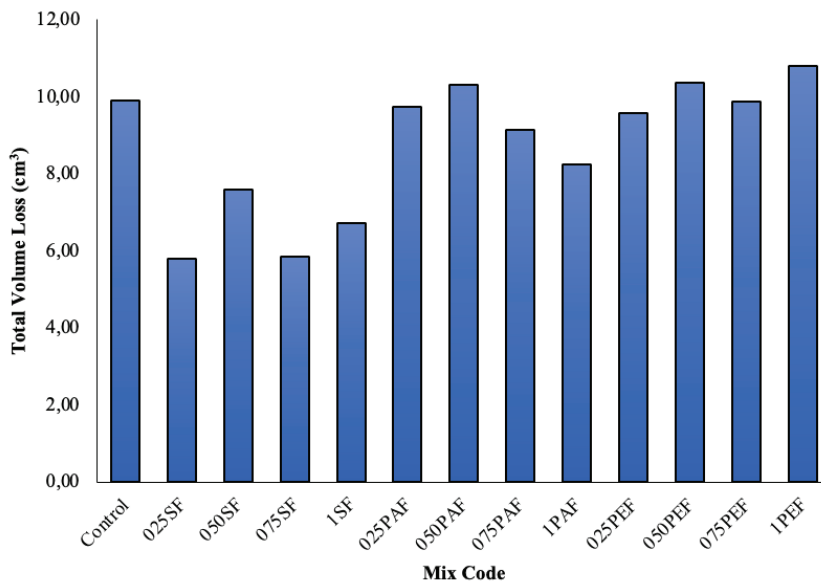


Figure 14. Abrasion resistance of GCs at 28 days.

the curing, the physical properties of the aggregate used, and the mixing ratios. Wear on surfaces: It can be caused by friction caused by factors such as sliding, scraping, or hitting. Concretes or composites should be homogeneous to prevent wear and pitting at different levels. In Figure 14 where the 28-day abrasion resistances are given, it is seen that the total volume loss in SF-GC samples after wear is lower than in the control and synthetic fiber-GCs. However, lower losses were obtained compared to the control with other fibers, where

there was more total volume loss than in the SF-GC samples. In general, total volume loss decreased for increasing ratios of PAF reinforcement with SF-GC series, but volume loss did not change much with PEF-reinforcement at all ratios. The loss with the control samples was 9.91 cm<sup>3</sup>, while the highest loss relative to the GC0 for the three batches in synthetic fiber-GCs was only 8.32%. For the 025SF and 075SF series, where the best results were acquired, the mean loss was reduced by 41.13% compared to the control.

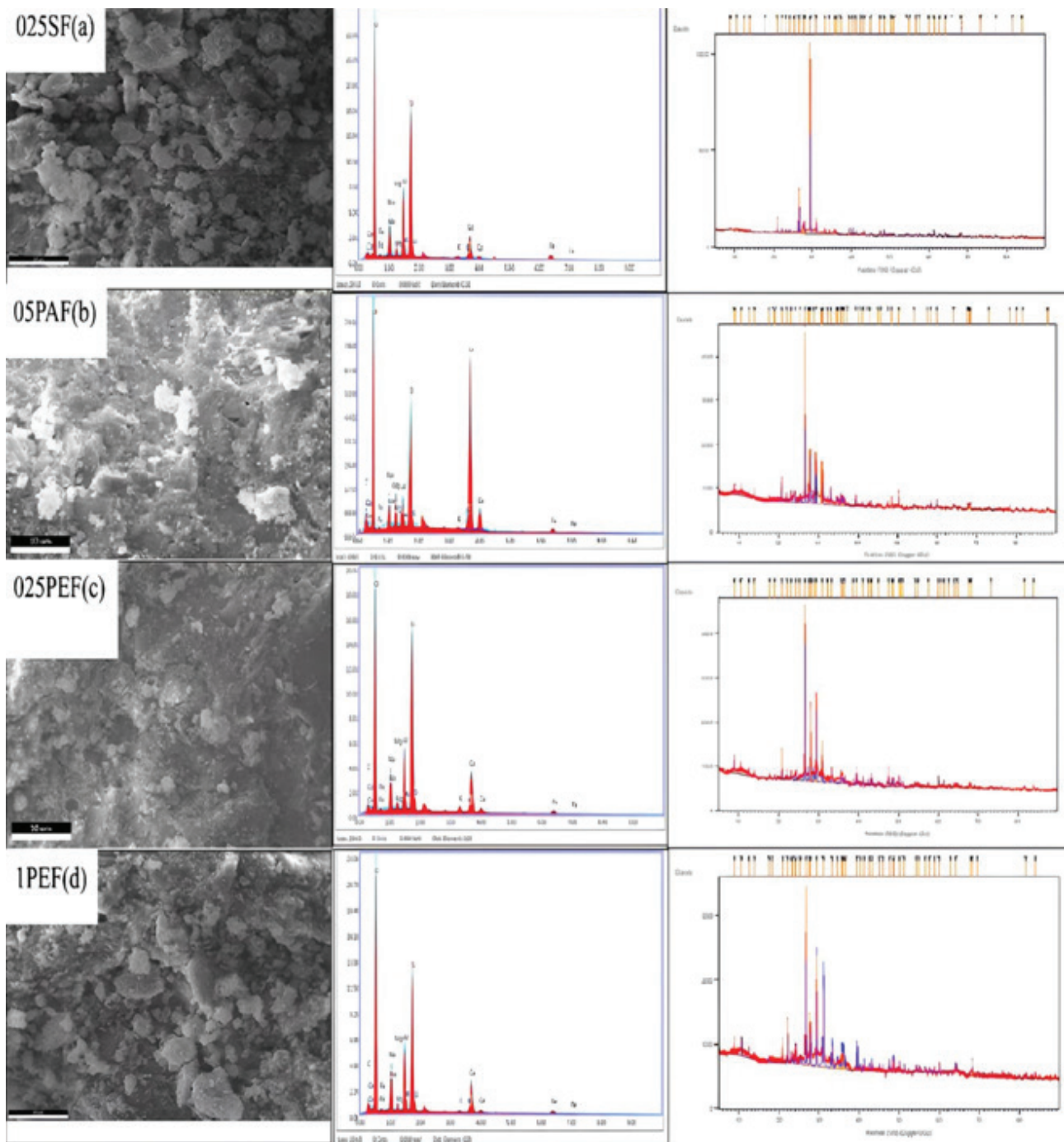


Figure 15. Microstructural analyses in GCs (025SF (a), 050PAF (b), 025PEF (c), and 1PEF (d))C.

### Microstructural Analysis

This Figure 15 provides microstructural analysis (SEM, EDS, XRD) of selected GCs exposed to high temperatures. It shows the microstructural integrity, elemental composition, and phase analysis of the GCs, illustrating how fiber reinforcement and the incorporation of industrial by-products like BP and RCA contribute to the overall stability and durability of the composites. In this study, SEM, EDS, and XRD analyses were performed on GCs, which were exposed to high temperature after 28 days and obtained the best strength and durability (Fig. 15.). Components of the binders consist of amorphous phases of  $\text{Al}_2\text{O}_3$  and  $\text{SiO}_2$ , which are widely used due to their remarkable mechanical and durability properties. Despite some unreacted precursors in SEM analyses, a stable and continuous structure of the GC matrix stands out. However, microfibrils of fiber-reinforced GCs are seen at 5000x magnification in all SEM-EDS analyses. In the series with 025SF, there is no obvious deformation on the surface, as well as 025PEF, 050PAF, and 1PEF. In EDS analysis, Si, Al, Na, Ca, and O elements, the prominent peaks of GCs, were observed. In addition, Ca, C, and O peaks were investigated for developing and non-developing samples. Results demonstrated that the peaks of the significant elements of  $\text{CaCO}_3$  were higher in the developed samples than in the undeveloped ones. When the ITZ between the aggregate and the matrix caused by RCA in some parts is lost, the strength of GCs may decrease. In addition, thermal expansion of aggregates due to high temperature can lead to cracks due to internal stresses, but these effects have been tried to be limited to fibers. Uysal et al. (2023) revealed an excellent geopolymerization between RM-MK-BP-RCA and alkaline solutions in the microstructural analysis of GCs. Although BF and PEFs have a good interface with the matrix, they show weak bonding, whereas glass and PVAFs have matrix-fiber strong bonds. Sahin et al. (2021) displayed a concordance between high temperature, freezing-thawing, and abrasion resistance results and SEM images, and the stability of the samples is preserved. Similar to the study, it was observed that the only loss was the stability of the RCA after 800°C.

According to XRD analysis, quartz peaks were found in the structure of GCs, and the percentage of crystalline silica was high in the filling materials used. While the  $\text{SiO}_2$  peaks are most concentrated in the sequence of  $20^\circ$ - $30^\circ$   $2\theta$ , it has been found that there is an effective geopolymerization in this band. Using RCAs,  $\text{NO}_3^-$ s, and  $\text{CaCO}_3$ s combined with mullite at low peaks have emerged. It has been revealed that crystallized C-S-H is created withal  $\text{CaCO}_3$  in all doped-undoped GCs by reacting appropriately with the Si-O-Al structure of  $\text{Na}^+$ . In the GC series, along with quartz, there are peaks in trace amounts of mullite and calcite. Different characteristic peaks may be due to mixture designs, binder type, coarse or fine aggregate type, alkalis, unreacted alumina, silica, or other reacted elements.

### CONCLUSIONS

Relevant studies in GC technology, mainly on brick dust and other industrial wastes, are limited. In this context, while various fibers such as BP, GBFS, FA, MK, and BP as waste materials are included in different fiber volumes, this study aims to evaluate construction waste as fine aggregate. Extensive physical, mechanical, and durability tests have been carried out on these mixtures, and the conclusions are given below;

While determining the physical properties of the samples before and after the durability effects, it was observed that the unit weights at 28 days compared to the control increased with the SF-reinforcement and its ratio and decreased with the PAF and PEF reinforcement. However, in the case that the void ratios decreased with PAF and PEF reinforcement in 7 days but increased with SF reinforcement, the void ratios increased in all samples of PEF reinforcement in 28 days. In the series, the increment was found to be 1.84%. Similarly, it was observed that the change in unit weights of the samples was limited (0.575%) after two different sulfate effects. In comparison, the void ratios rose by a maximum of 6.11% after the  $\text{Na}_2\text{SO}_4$  solution. However, in the  $\text{Mg}_2\text{SO}_4$  solution, the void ratio decreased in all series, unlike the control, and the best result was obtained in the 1PEF series, with a decline of approximately 31.08%.

Compared to the control, the most successful results for compressive strength with fiber reinforcement were obtained with the addition of 0.50% SF, 1% PAF, and 1% PEF. At the same time, the situation was different for sSFs in flexural strengths, and the best series was found to be 1SF. Flexural strength rises with increased fiber reinforcement and is attributed to the bond strength developed between fiber matrix and crack bridging behavior. However, using these fibers at higher ratios may cause a decrease in compressive and flexural strengths due to the agglomeration of the fibers and reduce their workability.

According to the compressive strengths obtained after the freezing-thawing effect, an increase was sighted in all GCs compared to the control, while the best series were 025SF and 1PAF. However, it was observed that the strength increased with the rise of fiber reinforcement in the series in terms of flexural strengths. For the compressive strength of the samples after the freezing-thawing, there was a loss of strength of approximately 37.5% in control, while the loss was 23%, 16.67%, and 12.5%, respectively, in the best series with SF, PEF, and PAF reinforcement. Based on the results, the best fiber order after freezing-thawing among the fibers was PEF> PAF>SF. On the other hand, not much decrease was observed after the effect, including the control series, and the average loss for all samples remained approximately 12.5%.

After the high temperature of the samples at the end of 28 days, there was a decrease at 300 °C in the control and fiber-reinforced GC series according to the compressive

strength losses. After 300 °C, the average loss was 16.8% in the other samples, excluding the SF series, while the strength gain was approximately 10.81% for 05SF, the series with the best SF reinforcement. For the flexural results, which increased with fiber reinforcement, the strength loss in the series with 1SF increased by approximately 2.98 times compared to the compressive. Similarly, while the loss of flexural strength decreased by approximately 50% in the series with 075PAF, the loss remained at a deficient level of 3.85% in the series with 050PEF. Compared to 300 °C at a temperature of 600 °C, the maximum 68.75% compressive strength loss, while the flexural strength decreased by 75%. At this temperature, the compressive and flexural strengths of the control and fibrous series are seriously reduced. Unlike the others, while the best series were obtained with control and 0.75% PEF-reinforcement, the structural strength condition was also met, and the average of the minimum compressive strength loss average was 34.16% for both.

When the results of the compressive and flexural strength of the samples after both sulfate effects are considered, there was a decrease in strength after 180 days. However, in the study in which the effect of sodium sulfate was compared with the effect of  $Mg_2SO_4$ , no difference was observed in compressive strengths. However, the effect of  $Mg_2SO_4$  was devastating in terms of flexural strengths. In the samples in  $Na_2SO_4$  solution, strengths very close to the control series were obtained with 0.25% metal and synthetic fiber reinforcement regarding compressive strength. In contrast, strengths were lower than the control in other fiber ratios. However, for the samples kept in  $Mg_2SO_4$  solution, 025SF was the only series that passed the control in distribution, while the closest result was obtained with the 075PEF series. However, when the flexural strengths of both solutions were compared to the control, it was observed that all fibered series increased significantly. While the series with the best strength after the  $Mg_2SO_4$  solution was 075PAF > 075PEF > 025SF, respectively, after the  $Na_2SO_4$  solution, it was observed that the flexural strengths increased gradually with fiber reinforcement up to 1% for both metal and synthetic fiber series. In the  $Na_2SO_4$  solution, the best series of flexural strength was 1PEF compared to the control, while the rise in strength was approximately 31.25%.

With the addition of synthetic fibers to the GC samples, the wear resistance increased, albeit partially, compared to the control. In contrast, the rise in wear resistance was evident when SF was added, and the best results were obtained in the 075SF series. While it was observed that the total volume loss decreased by approximately 40.40% in this series compared to the control, the total volume loss for the 1SF series increased by 2.84% compared to the 075SF series. A similar trend was observed with fiber reinforcement, while weight loss was also detected after all the effects.

There is a correlation between the compressive-flexural strength of the GC samples according to the UPVs. However, as the transition rates increased with age, the

UPV values of the PAF series with control at all fiber ratios remained almost the same at 90 days. While the highest UPV obtained with the 025SF series from the metal fiber was 3004 m/s, the best series was found with 075SF after durability effects, and the value was 3125 m/s. Considering all mixtures in terms of synthetic fibers, the highest UPV was 3311 m/s after the effects in the 1PAF series. In contrast, the best series was found to be 050PEF before and after the effects of PEF reinforcement, and the UPVs were 2874 and 3289 m/s, respectively.

Findings of the research indicate that the incorporation of fibers such as steel, polyamide, and polyethylene into GCs results in significant enhancements in mechanical properties and durability, rendering these materials highly suitable for practical applications in the construction industry and sustainable building practices. The fiber-reinforced GCs exhibit exceptional compressive and flexural strengths and improved toughness, crucial for ensuring resilience against environmental stressors such as freeze-thaw cycles, sulfate exposure, and high temperatures. For example, the composites have demonstrated superior performance in retaining structural integrity and mechanical properties under these harsh conditions, which is essential for the longevity and reliability of infrastructure projects. In addition to the mechanical benefits, the use of industrial by-products, such as metakaolin, fly ash, slag, red mud, brick powder, and recycled concrete aggregate, in the synthesis of GCs offers significant environmental advantages. Often considered waste, these materials are effectively recycled and utilized, reducing the carbon footprint and overall environmental impact of construction activities. This approach is consistent with the tenets of the circular economy. This approach to synthesizing GCs promotes sustainable development by minimizing the need for virgin raw materials and reducing greenhouse gas emissions associated with traditional Portland cement production. The practical implications of these findings are considerable. Fiber-reinforced GCs enhanced durability and mechanical properties permit their use in various demanding applications, including bridges, highways, and high-rise buildings, where long-term performance and resilience are critical. The capacity of these composites to withstand extreme environmental conditions without significant degradation ensures that they provide a durable and reliable alternative to conventional construction materials.

Moreover, the environmental advantages associated with using recycled materials in GCs assist in fulfilling rigorous regulatory standards for sustainable construction and contribute to broader environmental sustainability objectives. In conclusion, implementing fiber-reinforced GCs in construction projects can transform the industry by providing high-performance, eco-friendly alternatives to traditional cement-based materials. These advancements support the development of more resilient and sustainable infrastructure, which aligns with global trends towards greener building practices and the efficient use of

resources. Consequently, fiber-reinforced GCs represent a promising solution for addressing modern construction challenges, offering enhanced performance and environmental sustainability.

## FUTURE RESEARCH

**Long-term Performance Studies:** Conduct extensive field studies to gather long-term performance data under various environmental conditions. This includes assessing durability, structural integrity, and resistance to environmental factors such as freeze-thaw cycles, chemical exposure, and varying load conditions over extended periods.

**Standardization of Materials:** Develop standardized processing techniques and quality control measures for BP and RCA to ensure consistent performance and reliability of GCs. Establishing industry-wide standards and guidelines will facilitate uniformity and increase trust among manufacturers and end-users.

**Optimization of Mix Design:** Explore various proportions and combinations of BP, RCA, and other supplementary materials to optimize the mechanical properties, durability, and cost-effectiveness of the composites. Experimental studies to identify the optimal mix designs will help balance performance and sustainability, considering factors such as compressive strength, flexural strength, and workability.

**Scaling Up Production:** Investigate scalable manufacturing processes for producing GCs with recycled materials on an industrial scale. Address potential challenges in mass production to ensure the processes remain economically viable and environmentally friendly. Examine the feasibility of implementing large-scale production techniques and their impact on sustainability.

**Lifecycle Analysis and Sustainability:** Perform comprehensive lifecycle assessments to evaluate the environmental impact, sustainability, and economic viability of GCs with BP and RCA compared to conventional construction materials. These assessments should consider the entire lifecycle, from raw material extraction and production to usage and end-of-life disposal, providing a holistic view of their benefits and limitations.

**Innovative Applications:** Explore new and innovative applications for GCs with BP and RCA in various construction sectors, including infrastructure projects, residential and commercial buildings, and the repair and rehabilitation of existing structures. Research should focus on demonstrating the practical benefits of these composites in different contexts, highlighting their versatility and performance advantages.

**Advanced Technologies:** Integrate advanced technologies, such as intelligent monitoring systems and sensors, into GCs to enhance their functionality and performance. These technologies can provide real-time data on the condition and performance of the composites, enabling

proactive maintenance and improving the overall lifespan of structures.

**Economic Analysis:** Conduct detailed economic analyses to compare the costs and benefits of using GCs with BP and RCA against traditional materials. Evaluate initial production costs, long-term maintenance savings, and potential economic incentives for using sustainable materials in construction.

**Petrographic Analysis:** Implement petrographic analysis to study GCs microstructure and mineralogical composition. This will provide insights into the composites' bonding mechanisms, durability, and performance characteristics, helping optimize the mix design and improve material properties.

**Biotechnological Enhancements:** Investigate biotechnological methods, such as incorporating bacteria for self-healing properties in GCs. This could enhance the durability and longevity of the composites by enabling them to repair cracks and other minor damages autonomously.

**Nanotechnology:** Explore the application of nanotechnology to enhance the properties of GCs. Incorporating nanomaterials can improve mechanical strength, thermal stability, and durability, making the composites even more robust and versatile for various construction applications.

Furthermore, future research should also investigate the potential of advanced mathematical and optimization models to enhance the performance of GCs. For instance, utilizing fuzzy ranking functions may prove advantageous in optimizing material properties in complex systems. Sharma et al. [48] demonstrated the effectiveness of a Fermatean fuzzy ranking function in optimizing intuitionistic fuzzy transportation problems, thereby highlighting the potential for similar approaches to be applied in optimizing material properties in GCs. Integrating such sophisticated fuzzy models can facilitate a comprehensive assessment and enhancement of these composites' mechanical and durability properties. Furthermore, Bayesian models can be utilized to predict and analyze the variability in material characteristics, thereby affording more precise control over the production process. For example, Vandana et al. [49] employed Bayesian models to forecast art prices, and their methodology can be adapted to predict the performance of GCs under different conditions. The application of Bayesian approaches enables researchers to account for uncertainty and variability in material properties, thereby facilitating the development of more reliable and optimized production methods. Moreover, investigating novel types of weak open sets via idealization in bitopological spaces can provide innovative analytical tools for analyzing the structural and functional properties of GCs. Sharma et al. [50] introduced a novel type of weak open sets in topological spaces, which can be utilized to elucidate the microstructural behaviors and interactions of GCs. Such sophisticated mathematical frameworks can offer deeper insights into the material properties and facilitate the development of more robust and efficient composites. These advanced

mathematical models and techniques can significantly contribute to optimizing and understanding GCs, providing a theoretical foundation for future research and practical applications. By integrating these sophisticated analytical tools, researchers can develop more effective strategies for improving the performance and sustainability of GCs.

## DATA AVAILABILITY

The data supporting this study's findings are available from the corresponding author, [Beyza Fahriye AYGUN], upon reasonable request.

## REFERENCES

- [1] Sahin F, Uysal M, Canpolat O, Cosgun T, Dehghanpour H. The effect of polyvinyl fibers on metakaolin-based geopolymer mortars with different aggregate filling. *Constr Build Mater* 2021;300:124257. [\[CrossRef\]](#)
- [2] Ipek S, Ekmen S. Investigation of recycling of building materials as sand in the production of geopolymer mortar. *Adiyaman Univ J Eng Sci* 2022;17:404–419. [\[CrossRef\]](#)
- [3] Lakew A, Canpolat O, Al-Mashhadani M, Uysal M, Nis A, Aygörmez Y, Bayati M. Combined effect of using steel fibers and demolition waste aggregates on the performance of fly ash/slag based geopolymer concrete. *Eur J Environ Civ Eng* 2023;27:1–28. [\[CrossRef\]](#)
- [4] Li Y, Shen J, Lin H, Lv J, Feng S, Ci J. Properties and environmental assessment of eco-friendly brick powder geopolymer binders with varied alkali dosage. *J Build Eng* 2022;58:104975. [\[CrossRef\]](#)
- [5] Migunthanna J, Rajeev P, Sanjayan J. Investigation of waste clay brick as partial replacement in geopolymer binder. *Constr Build Mater* 2023;365:130132. [\[CrossRef\]](#)
- [6] Uysal M, Aygörmez Y, Canpolat O, Cosgun T, Kuranlı ÖF. Investigation of using waste marble powder, brick powder, ceramic powder, glass powder, and rice husk ash as eco-friendly aggregate in sustainable red mud-metakaolin based geopolymer composites. *Constr Build Mater* 2022;361:129627. [\[CrossRef\]](#)
- [7] Liu J, Doh J, Ong D, Dinh H, Podolsky Z, Zi G. Investigation on red mud and fly ash-based geopolymer: Quantification of reactive aluminosilicate and derivation of effective Si/Al molar ratio. *J Build Eng* 2023;71:106457. [\[CrossRef\]](#)
- [8] Liang X, Ji Y. Mechanical properties and permeability of red mud-blast furnace slag-based geopolymer concrete. *SN Appl Sci* 2021;3:1–11. [\[CrossRef\]](#)
- [9] Nazir K, Canpolat O, Uysal M, Nis A, Kuranlı Ö. Engineering properties of different fiber-reinforced metakaolin-red mud based geopolymer mortars. *Constr Build Mater* 2023;385:131630. [\[CrossRef\]](#)
- [10] Celik A, Yilmaz K, Canpolat O, Al-Mashhadani M, Aygörmez Y, Uysal M. High-temperature behavior and mechanical characteristics of boron waste additive metakaolin based geopolymer composites reinforced with synthetic fibers. *Constr Build Mater* 2018;187:1190–1203. [\[CrossRef\]](#)
- [11] Zhong H, Zhang M. Effect of recycled tyre polymer fibre on engineering properties of sustainable strain hardening geopolymer composites. *Cem Concr Compos* 2021;122:104155. [\[CrossRef\]](#)
- [12] Alomayri T, Low IM. Synthesis and characterization of mechanical properties in cotton fiber-reinforced geopolymer composites. *J Asian Ceram Soc* 2013;1:30–34. [\[CrossRef\]](#)
- [13] Alomayri T, Shaikh FUA, Low IM. Characterisation of cotton fibre-reinforced geopolymer composites. *Compos B Eng* 2013;50:1–6. [\[CrossRef\]](#)
- [14] Liu J, Doh J, Ong D, Dinh H, Podolsky Z, Zi G. Investigation on red mud and fly ash-based geopolymer: Quantification of reactive aluminosilicate and derivation of effective Si/Al molar ratio. *J Build Eng* 2023;71:106457. [\[CrossRef\]](#)
- [15] Shaikh FUA. Tensile and flexural behaviour of recycled polyethylene terephthalate (PET) fibre reinforced geopolymer composites. *Constr Build Mater* 2020;245:118424. [\[CrossRef\]](#)
- [16] Smith J, Doe A, Johnson L. Properties and applications of fiber-reinforced geopolymer composites. *J Mater Sci* 2022;57:3412–3421.
- [17] Jones M, Brown R. Durability of geopolymer composites in aggressive environments. *Constr Build Mater* 2021;293:123456.
- [18] Williams P, Zhao Q, Kumar R. Mechanical performance of geopolymer composites with recycled aggregates. *Cem Concr Res* 2023;155:105345.
- [19] Davis S, Patel K. Influence of fiber type on the properties of geopolymer composites. *Mater Des* 2020;192:109876.
- [20] Martin J, Liu H. Sustainability of geopolymer composites incorporating industrial by-products. *J Clean Prod* 2021;290:125678.
- [21] Zhang L, Wang S, Cheng Y. Microstructure and mechanical properties of fly ash-based geopolymer. *Constr Build Mater* 2020;250:118340.
- [22] Chen Y, Gao T. Performance of geopolymer concrete under severe environmental conditions. *J Build Eng* 2021;44:103554.
- [23] Lee B, Kim H, Park J. Advances in geopolymer composites for structural applications. *Compos B Eng* 2022;230:109824.
- [24] Singh S, Aswath M, Ranganath R. Performance assessment of bricks and prisms: Red mud based geopolymer composite. *J Build Eng* 2020;32:101690. [\[CrossRef\]](#)
- [25] Aygörmez Y. Evaluation of the red mud and quartz sand on reinforced metazeolite-based geopolymer composites. *J Build Eng* 2021;43:102886. [\[CrossRef\]](#)

- [26] Zakira U, Zheng K, Xie N, Birgisson B. Development of high-strength geopolymers from red mud and blast furnace slag. *J Clean Prod* 2023;383:135484. [\[CrossRef\]](#)
- [27] Gomes Silveira N, Figueiredo Martins M, Bezerra A, Gabriel da Silva Araújo F. Ecological geopolymer produced with a ternary system of red mud, glass waste, and Portland cement. *Clean Eng Technol* 2022;6:100379. [\[CrossRef\]](#)
- [28] Kuranlı ÖF, Uysal M, Abbas M, Cosgun T, Nis A, Aygörmez Y, Al-Mashhadani M. Evaluation of slag/fly ash based geopolymer concrete with steel, polypropylene and polyamide fibers. *Constr Build Mater* 2022;325:126734. [\[CrossRef\]](#)
- [29] Zhao Q, Wang Y, Xie M, Huang B. Experimental study on mechanical behavior of steel fiber reinforced geopolymeric recycled aggregate concrete. *Constr Build Mater* 2022;356:129282. [\[CrossRef\]](#)
- [30] Bellum R. Influence of steel and PP fibers on mechanical and microstructural properties of fly ash-GGBFS based geopolymer composites. *Ceram Int* 2022;48:6808–6818. [\[CrossRef\]](#)
- [31] Aisheh Y, Atrushi D, Akeed M, Qaidi S, Tayeh B. Influence of polypropylene and steel fibers on the mechanical properties of ultra-high-performance fiber-reinforced geopolymer concrete. *Case Stud Constr Mater* 2022;17:e01602. [\[CrossRef\]](#)
- [32] Mudgal M, Singh A, Chouhan R, Acharya A, Srivastava A. Fly ash red mud geopolymer with improved mechanical strength. *Clean Eng Technol* 2021;4:100212. [\[CrossRef\]](#)
- [33] Qian L, Ahmad M, Lao J, Dai J. Recycling of red mud and flue gas residues in geopolymer aggregates (GPA) for sustainable concrete. *Resour Conserv Recycl* 2023;191:106858. [\[CrossRef\]](#)
- [34] Uysal M, Kuranlı ÖF, Aygörmez Y, Canpolat O, Cosgun T. The effect of various fibers on the red mud additive sustainable geopolymer composites. *Constr Build Mater* 2023;363:129932. [\[CrossRef\]](#)
- [35] Dhasindrakrishna K, Pasupathy K, Ramakrishnan S, Sanjayan J. Rheology and elevated temperature performance of geopolymer foam concrete with varying PVA fibre dosage. *Mater Lett* 2022;328:133072. [\[CrossRef\]](#)
- [36] Zhang P, Han X, Hu S, Wang J, Wang T. High-temperature behavior of polyvinyl alcohol fiber-reinforced metakaolin/fly ash-based geopolymer mortar. *Compos B Eng* 2022;244:110151. [\[CrossRef\]](#)
- [37] Zheng X, Zhang J, Ding X, Chu H, Zhang J. Frost resistance of internal curing concrete with calcined natural zeolite particles. *Constr Build Mater* 2021;288:123107. [\[CrossRef\]](#)
- [38] Jiao Z, Li X, Yu Q. Effect of curing conditions on freeze-thaw resistance of geopolymer mortars containing various calcium resources. *Constr Build Mater* 2021;313:125589. [\[CrossRef\]](#)
- [39] Elyamany H, Abd Elmoaty A, Elshaboury A. Magnesium sulfate resistance of geopolymer mortar. *Constr Build Mater* 2018;184:111–127. [\[CrossRef\]](#)
- [40] Zada Farhan K, Azmi Megat Johari M, Demirboğa R. Evaluation of properties of steel fiber reinforced GGBFS-based geopolymer composites in aggressive environments. *Constr Build Mater* 2022;345:128296. [\[CrossRef\]](#)
- [41] Guo X, Xiong G. Resistance of fiber-reinforced fly ash-steel slag based geopolymer mortar to sulfate attack and drying-wetting cycles. *Constr Build Mater* 2021;269:121329. [\[CrossRef\]](#)
- [42] Kuri J, Nuruzzaman M, Sarker P. Sodium sulphate resistance of geopolymer mortar produced using ground ferronickel slag with fly ash. *Ceram Int* 2023;49:2765–2773. [\[CrossRef\]](#)
- [43] Sata V, Sathonsaowaphak A, Chindaprasirt P. Resistance of lignite bottom ash geopolymer mortar to sulfate and sulfuric acid attack. *Cem Concr Compos* 2012;34:700–708. [\[CrossRef\]](#)
- [44] Supit S, Olivia M. Compressive strength and sulfate resistance of metakaolin-based geopolymer mortar with different ratio of alkaline activator. *Mater Today Proc* 2022;66:2776–2779. [\[CrossRef\]](#)
- [45] Obeng J, Andrews A, Adom-Asamoah M, Adjei S. Effect of calcium carbide residue on the sulphate resistance of metakaolin-based geopolymer mortars. *Clean Mater* 2023;7:100188. [\[CrossRef\]](#)
- [46] Kwasny J, Aiken T, Soutsos M, McIntosh J, Cleland D. Sulfate and acid resistance of lithomarge-based geopolymer mortars. *Constr Build Mater* 2018;166:537–553. [\[CrossRef\]](#)
- [47] Yang W, Liu H, Zhu P, Zhu X, Liu X, Yan X. Effect of recycled coarse aggregate quality on the interfacial property and sulfuric acid resistance of geopolymer concrete at different acidity levels. *Constr Build Mater* 2023;375:130997. [\[CrossRef\]](#)
- [48] Sharma MK, Sadhna AK, Bhargava S, Kumar L, Rathour LN, Mishra S, Pandey S. A Fermatean fuzzy ranking function in optimization of intuitionistic fuzzy transportation problems. *Adv Math Model Appl* 2022;7:191–204.
- [49] Vandana, Deepmala K, Drachal LN, Mishra LN. Forecasting art prices with Bayesian models. *Thai J Math* 2021;19:479–491.
- [50] Sharma DJ, Kilicman A, Mishra LN. A new type of weak open sets via idealization in bitopological spaces. *Malays J Math Sci* 2021;15:189–197.